The EUMETSAT Network of Satellite Application Facilities

NWC SAF

Support to Nowcasting and Very Short Range Forecasting

Studies for the use of MTG-IRS L1 in nowcasting based in validation and training activities of the NWCSAF clear air products

NWC/CDOP2/GEO/AEMET/SCI/RP/02, Issue 1, Rev. 0

30 November 2014

Prepared by AEMET

REPORT SIGNATURE TABLE

Function	Name	Signature	Date
Prepared by	Miguel A. Martínez (AEMET)		*30 November 2014*
Reviewed by	Javier Garcia-Pereda (AEMET)		*30 November 2014*
Authorised by	Pilar Rípodas SAFNWC Project Manager		*30 November 2014*

DOCUMENT CHANGE RECORD

Version	Date	Pages	CHANGE(S)
1.0	30 November 2014	23	

Table of contents

List of Tables and Figures

1. INTRODUCTION

The Eumetsat “Satellite Application Facilities” (SAF) are dedicated centres of excellence for processing satellite data, and form an integral part of the distributed EUMETSAT Application Ground Segment (http://www.eumetsat.int). This documentation is provided by the SAF on Support to Nowcasting and Very Short Range Forecasting, NWC SAF. The main objective of NWC SAF is to provide further develop and maintain software packages to be used for Nowcasting applications of operational meteorological satellite data by National Meteorological Services. More information can be found at the NWC SAF webpage, http://www.nwcsaf.org. This document is applicable to the NWC SAF processing package for Meteosat meteorological satellites, SAFNWC/MSG.

1.1 PURPOSE

When designing the CDOP phase, it was considered necessary to foresee the WP 6120 [AD.1] "MTG algorithm for Clear Air Products" to be executed at the end of the CDOP to calculate proxy data for the future MTG-FCI. This WP was needed because the design of MTG program was not fixed when the NWC SAF Proposal for CDOP phase was written in 2006.

WP 6120	**Title: MTG algorithm studies for Clear Air Products**			
	Comments:			
Start: End of MTG phase B (2009?)	**End:** Feb 2012	**Effort (m.m):** 4.0 + 9 VSA	**Cost:** 32,456 k€ +VSA	**Responsible partner:** INM
WP Content	*Objective:* To assess the applicability of the existing Clear Air algorithms to MTG. *Tasks:* *) Evaluation of the channels available in MTG instruments. *) Identification of key algorithm studies.			
WP Input	MTG documents			
WP Output	Scientific report			
WP Interfaces				
Interactions with other SAFS and/or Federated Activities	None			

Figure 1: Original formulation of WP 6120.

Since the final selection of IR channels for MTG-FCI was near equivalent to the MSG ones (MTG-FCI IR and WV channels have similar central wavelength to the MSG ones) this WP had not sense for the MTG-FCI instrument. Also at the end of CDOP phase there were not available spectral response functions for MTG-FCI and there were not available MTG-FCI RTTOV coefficients.

One alternative way to get proxy data was the use of IASI synthetic brightness temperatures (hereafter BTs) and then to create pseudo MTG-FCI BTs datasets with different spectral response functions. The idea to compare different MTG-FCI BTs from different MTG-FCI spectral response functions was considered as not useful. But the calculation of synthetic IASI BTs was considered as very interesting in order to anticipate the use of MTG-IRS in nowcasting and how the NWC SAF could be prepared for the MTG-IRS era.

In 2010, PGE13 validation and training software were modified in order to compute IASI BTs using RTTOV and ECMWF profiles. This PGE13 validation and training software is described in [RD.1] and [RD.2]. After solving some technical problems related to the huge memory size and huge files size needed, need of 64 bits machine and other technical problems, the synthetic IASI BTs for an ECMWF GRIB analysis were first obtained in 2010. Then the use of an IASI to MTG-IRS conversion tool (Tjemkes and Calbet, 2008) allowed the generation of synthetic MTG-IRS BTs datasets in summer 2010. These activities were reported in [AD.3].

The first use of these synthetic hyperspectral BTs datasets was the pioneering generation of synthetic RGB images for MTG-IRS in 2010. It was published in the second part of (Martinez et al., 2010a).

In 2012, two presentations were made in the MIST framework pioneering the potential use of hyperspectral L1 data directly by forecasters. In 2013, the evolution of the ideas, developments and studies described in this report were presented on the Nowcasting Applications using MTG-IRS Workshop that took place in EUMETSAT Headquarter in 25 July 2013 and a summary was presented in a poster in the 2013 EUMETSAT Conference in Vienna; see (Martinez and Calbet, 2013).

1.2 Scope of the document

The works, studies and ideas described in this report will help to implement NWC SAF use of MTG-IRS Level 1. These studies are also valuable to anticipate the new ways that MTG-IRS Level 1 and Level 2 products could be used in MTG-IRS era for nowcasting and the synergies with MTG-FCI ones.

1.3 Definitions, Acronyms and Abbreviations

AEMET	Agencia Estatal de Meteorología
BT	Brightness temperatures
EUMETSAT	European Organisation for the Exploitation of Meteorological Satellites
FCI	Flexible Combined Imagery
IRS	InfraRed Sounder
MIST	Meteosat Third Generation InfraRed Sounder Team
MSG	Meteosat Second Generation
MTG	Meteosat Third Generation
NWC SAF	Satellite Application Facility for Nowcasting
NWP	Numerical Weather Prediction
SEVIRI	Spinning Enhanced Visible and Infrared Imager

1.4 References

1.4.1 Applicable Documents

The following documents, of the exact issue shown, form part of this document to the extent specified herein. Applicable documents are those referenced in the Contract or approved by the Approval Authority. They are referenced in this document in the form [AD.X].

For dated references, subsequent amendments to, or revisions of, any of these publications do not apply. For undated references, the current edition of the document referred applies.

Reference	Title	Code	Vers	Date
[AD. 1]	Proposal For The Continuous Development And Operations Phase	SAF/NWC/CDOP/INM/MGT/PRO	2.2	07/08/2006
[AD. 2]	NWC SAF Project and Operations Plan for the CDOP	SAF/NWC/CDOP/INM/MGT/PL/MP	1.1	04/05/2011
[AD. 3]	CDOP NWC SAF Progress Report #07	SAF/NWC/CDOP/INM/MGT/RP/PGR/07	1.0	27/10/2010

Table 1: List of Applicable Documents

1.4.2 Reference Documents

The reference documents contain useful information related to the subject of the project. These reference documents complement the applicable ones, and can be looked up to enhance the information included in this document if it is desired. They are referenced in this document in the form [RD.X].

For dated references, subsequent amendments to, or revisions of, any of these publications do not apply. For undated references, the current edition of the document referred applies.

Reference	Title	Code	Vers	Date
[RD.1]	Algorithm Theoretical Basis Document for PGE13 “SEVIRI Physical Retrieval Product” (SPhR) v1.0	SAF/NWC/CDOP/INM/SCI/ATBD/13	1.0	21/05/2010
[RD.2]	Validation Report for PGE13 "SEVIRI Physical Retrieval Product" (SPhR) v1.0	SAF/NWC/CDOP/INM/SCI/VR/08	1.0	06/10/2010

Table 2: List of Referenced Documents

2. AIM OF THE STUDY

The traditional use of hyperespectral data is mainly related to NWP and physical retrieval algorithms. This has been motivated by the polar orbit and the spatial resolution of the current hyperespectral instruments. But in 2020, the next MTG-IRS on geostationary orbit with a spatial resolution of 4 km in the subsatellite point and 30 minutes temporal resolution will open new possibilities on the use of hyperespectral Level 1 data in nowcasting and other branches. In order to anticipate and foster the use of MTG-IRS in nowcasting applications and especially on cloudy pixels (where the NWP and physical retrieval algorithms may not be applied), some innovative ideas to use the MTG-IRS L1B data as an imagery instrument are shown here.

RGB images can be used as one early and basic product. RGB images from geostationary satellites have been a great aid for the weather forecasters, most notably in the field of nowcasting; MSG RGB images are routinely used by forecasters since several years. The main reason for this resides on the ability of the human eye to quickly comprehend image information, especially when the image is colour coded and the individual has been trained to interpret them. An added advantage is that RGB coded images are also quickly generated from the original image data directly provided by the satellite. They also provide a global coverage of the complete visible disk as seen from the satellite perspective. RGB images are widely used in loops of RGB images to monitor fast changes in the atmosphere; the use of loops is related to the ability of the human to detect very small changes in position and colour in colour images.

This study was initiated as a side training activity but it has evolved to the important issue related on the way of hyperspectral data could be used in nowcasting. In 2010, one poster was submitted to the training session of the 2010 EUMETSAT Conference in Cordoba. The aim of this poster was to demonstrate the utility of synthetic RGB imagery in training purposes in the sense that some airmass and dust MSG RGB issues could be illustrated.

Minor changes in the call to RTTOV routine were made in order to use ECMWF GRIB files as input and to allow modifications on zenith angle and other conditions (as example clear or cloudy pixel). The outputs were synthetic MSG RGB images with different zenith angle and conditions. These synthetic MSG BTs were used for synthetic MSG RGB generation for training purposes and some examples are shown in Figures 3 and 4. They were published in the first part of (Martinez et al., 2010a). Next step was the adaptation of this software to compute synthetic IASI BTs with the goal of completing the original WP6120 tasks.

There are hundreds of IASI channels inside the spectral range of each one of the MSG channels. For this reason, it was initiated a work to compare synthetic MSG IR BTs with synthetic IASI BTs to search the nearest IASI channels to MSG ones. The nearest IASI channels were used to obtain the first synthetic IASI RGB image and later the first MTG-IRS sounder RGBs. These pioneering images were generated in 2010 and are summarized in the second part of (Martinez et al., 2010a).

3. WORK WITH SYNTHETIC BTs

3.1 DESCRIPTION

The starting point was to calculate synthetic brightness temperatures for MSG and IASI. To achieve this, RTTOV-9.3 with the MSG and IASI coefficients were used to calculate synthetic brightness temperatures using as input the same ECMWF fields. Zenith angle equal to zero and no noise simplified assumptions were used as a first choice. The ECMWF GRIB file used in these early studies was the ECMWF analysis for 25th May 2009 at 12 UTC. This case study was selected by the Convection Working Group because thunderstorms extended over France, Belgium and Germany; more information on this case study is on (Martinez et al., 2010b).

In the next step, the synthetic IASI radiances were converted to MTG-IRS spectral resolution with a radiation converter tool built at EUMETSAT (Tjemkes, 2008). This tool transforms the 8461 RTTOV IASI channels into the MTG-IRS radiances (1738 channels). The process is shown in Figure 2.

Once the synthetic BTs datasets for MSG, IASI and MTG-IRS were built, the key point is the search of the IASI (or MTG-IRS) channels nearest to each one of the MSG IR channels.

The search of the optimal MTG-IRS channel that best reproduces a MSG IR channel has been made identifying the synthetic MTG-IRS channel that simultaneously meets a high correlation and a low RMSE with synthetic MSG RTTOV BTs calculated from the same ECMWF GRIB file and conditions. To do that, it has been calculated the correlation and RMSE between each one of the MSG channels and the MTG-IRS ones for all the pixels. The MTG-IRS channels with highest correlations and lowest RMSE with respect to the MSG ones are selected. To select these channels it was searched the MTG-IRS channels with largest value after multiplying the correlation and the normalized inverted RMSE. The normalization of RMSE was done subtracting the mean RMSE and then scaling from 0 (for RMSE greater than the mean RMSE values) to 1 (for the lowest values).

Similar process was repeated to search the IASI channels nearest to each one of the MSG IR channels.

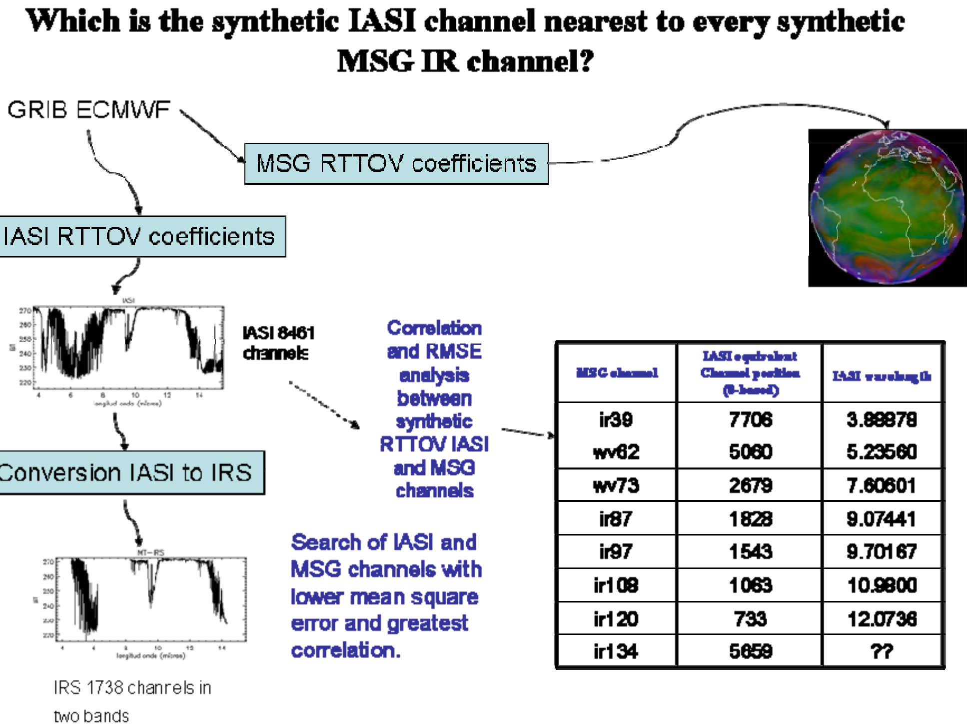

MSG channel	IASI equivalent Channel position (0-based)	IASI wavelength
ir39	7706	3.89978
wv62	5060	5.23560
wv73	2679	7.60601
ir87	1828	9.07441
ir97	1543	9.70167
ir108	1063	10.9800
ir120	733	12.0736
ir134	5659	??

Figure 2: Description of the process to calculate the synthetic IASI and MTG-IRS BTs.

The list of IASI channels nearest to each one of the MSG IR channels is shown in the Table inside Figure 2. The list of MTG-IRS channels that could be used instead of MSG ones is shown in Table 3.

It can be seen that the MSG substitutes for the water vapour channels are two MTG-IRS channels which are spectrally very close. The reason for this is that the high spectral resolution of MTG-IRS is able to separate individual water vapour lines. Thus, in MTG-IRS or IASI spectra two spectrally nearby channels could have very different absorptions. This channel correspondence should be contemplated as an initial first guess, because the atmospheric variability used is very low (only one GRIB file is used) and no noise has been introduced in the simulations. It just illustrates the technique to follow.

SEVIRI channel	Closest MTG-IRS channel number (0-based)	Closest MTG-IRS channel Wavelength (µm)
IR9.7	1723	4.6162
WV6.2	1122	5.5846
WV7.3	1231	5.3799
IR8.7	770	8.4656
IR9.7	519	9.7620
IR10.8	308	11.2045
IR12.0	201	12.1120

Table 3: List of MTG-IRS channels closest to MSG ones. This table has been used to built the MTG-IRS RGB images with MTG-IRS BTs instead of the closest MSG ones in the RGB recipes.

3.2 SYNTHETIC RGB IMAGES

RGB images provide good monitoring of spatial structures. Regular L2 retrieval algorithms are only applied over clear or over partly cloudy pixels. For this reason L2 products from regular algorithms generate images with parts of the image not processed. As a result, L2 images usually show isolated sets of pixels with a background colour. In these situations the human eye can lose the spatial structure over not processed regions. In the case of RGB imagery, all pixels have one RGB colour assigned; when loops of images are displayed the human eye is able to follow adequately the spatial structures.

Two main RGB images, derived from MSG and based on IR or WV channels, are widely used by forecasters operationally. These are the airmass RGB and the dust RGB. The airmass RGB is widely used in forecasting tasks. The dust RGB is used for several issues like dust monitoring and volcanic and SO_2 monitoring. More examples and documentation on the use of MSG RGBs can be seen in ***¡Error! Marcador no definido.***

The recipe for the airmass RGB composite can be seen in Table 4.

AIR MASS (night & day)					
RGB colour plane	channel (difference)	MIN	MAX	GAMMA	Prominent features
R	6.2 - 7.3	-25 K	0 K	1.0	(Rapid) cyclogenesis, jet streaks PV analysis Mid-level/high clouds
G	9.7 - 10.8	-40 K	+5 K	1.0	
B	6.2 (inverted!)	243 K	208 K	1.0	

Table 4: MSG airmass RGB composite construction (source: EUMETSAT RGB best practices document)

In Figure 3 one example of the comparison between one actual MSG airmass RGB and two synthetic RGB images (simulated with and without clouds) can be seen. The SEVIRI synthetic brightness temperatures have been calculated from the ECMWF analysis GRIB file for the same date with the RTTOV-9.3 version.

In Figure 4 several RGB images simulated without clouds using different zenith angles are shown. It can be observed a tendency to bluish colours in the RGB images with the increasing zenith angle. This illustrates the bad performance for high zenith angle and explains the bluish border of the images from Figure 3. This fact will be used in Section 4 to justify the possibility to generate RGB with actual IASI data on Polar Regions.

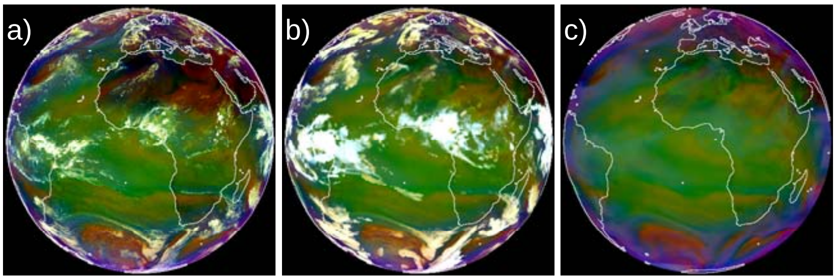

Figure 3: a) Actual MSG-2 airmass RGB, b) Synthetic cloudy RTTOV MSG from ECMWF analysis, c) Synthetic clear air RTTOV MSG from ECMWF analysis. The three images are from 25th May 2009 at 12 UTC

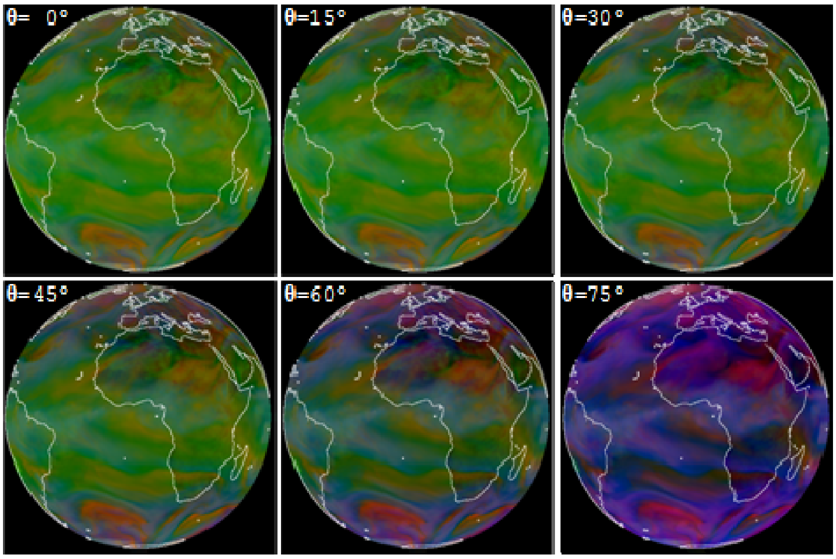

Figure 4: Clear RTTOV MSG airmass RGBs calculated with fixed zenith angles of 0º, 15º, 30º, 45º, 60º and 75º respectively.

3.3 SYNTHETIC IASI AND MTG-IRS AIRMASS RGB IMAGES

As first step the hyperspectral RGBs with MSG RGB heritage were built. MSG, IASI and MTG-IRS synthetic RTTOV BT channels were used to build the most frequently used RGB images.

MTG-IRS channels closest to the MSG channels (showed in Table 3) were used to generate the equivalent MSG airmass RGB imagery. IASI channels used to build the IASI RGB images can be looked up in the Table inside the Figure 2.

When comparing MSG airmass RGB image (Figure 5.left) versus MTG-IRS and IASI ones (Figure 5.center and Figure 5.right), it can be seen that the contrast in the MSG one is slightly lower. It is can be also seen that the MTG-IRS and IASI ones are slightly different. This is because the weighting functions are slightly different for the MTG-IRS and the IASI channels due to their different spectral positions and widths.

This experiment shows how radiative transfer models can explain some features of the airmass-RGB product, plus the possibilities opened by the new generation instruments on MTG IRS sounder.

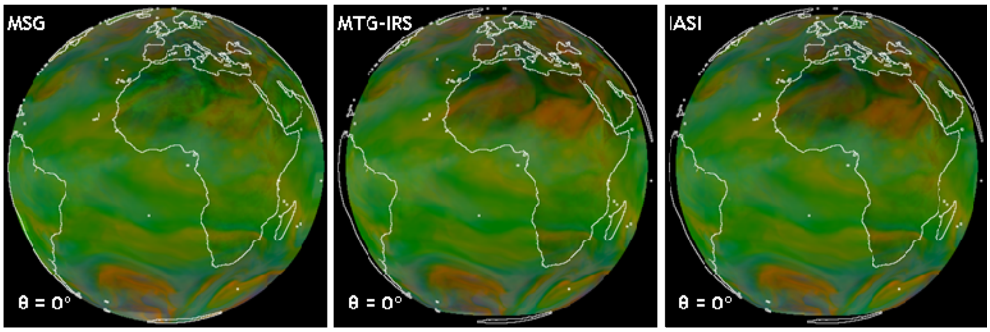

Figure 5: Clear synthetic RTTOV MSG (left), MTG-IRS (center) and IASI (right) airmass RGB calculated with zenith angle fixed to 0º using the MSG channels (left), MTG-IRS channels closest to MSG channels (center) and IASI ones (right)

4. ACTUAL IASI RGB IMAGES

Once synthetic RGB imagery have been built, as described in the previous section, the next step was to test them by building the same RGB imagery but with actual hyperspectral data.

Since MSG RGB imagery has good spatial and temporal resolution on the MSG full disk, it was better to explore the use of IASI RGB images over regions not covered by MSG. Thus, the first test was to explore the IASI RGB images on Polar region were the high zenith angle creates a bluish effect on MSG RGB images but not on IASI RGB images. It can be found in Section 6 a description of the processes to manage actual IASI files, to generate actual IASI RGB images and some issues related to an operational generation.

4.1 ACTUAL IASI RGB IMAGES ON POLAR REGIONS

An MSG airmass RGB showing the bluish colours over the disk border due to the high MSG zenith angles can be seen in Figure 6.left. When MSG RGB image is generated over the McIDAS-V Globe display, it is possible to move the globe to one Polar View (Figure 6.right) from the traditional Equatorial view (Figure 6.left).

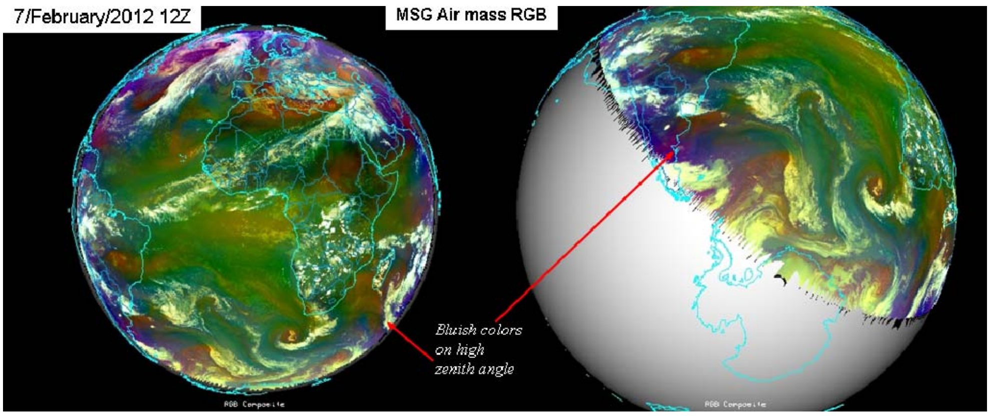

Figure 6: Left: 0º Geostationary view. Right: Antarctic view. Bluish colors on MSG pixels appear when zenith angle increases on MSG airmass RGB (disk MSG border).

In Figure 7, one IASI airmass RGB image was superimposed over the MSG airmass RGB images (pointed out by red arrows). From the comparison of IASI and MSG airmass RGB images on McIDAS-V Globe display it can be seen that on Polar Region there is an IASI airmass RGB coverage and that the IASI airmass RGB does not have the bluish colours. This effect is due to the fact that the IASI zenith angle is always low. IASI zenith angles vary only between the left and right edge in the range [-48º, 48º]. Thus IASI zenith angles on Polar Regions are lower than zenith angles from geostationary satellites. This fact allows a better contrast on RGB images in Polar

Regions from polar satellites since they are not affected by the high zenith angle on geostationary satellites.

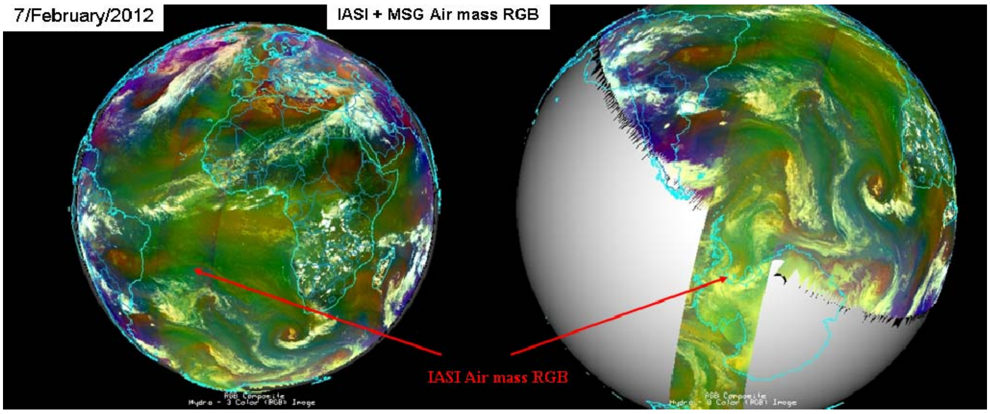

Figure 7: Left: 0º Geostationary view, Right: Antartic view. Bluish colors on MSG pixels appears when zenith angle increase on MSG Airmass RGB (disk MSG border on left image) but not on the pixels from IASI Airmas RGB where the IASI zenith angles are in range [-48º, 48º].

4.2 ACTUAL IASI RGB IMAGES ON GLOBAL COVERAGE

In order to promote the use of IASI RGBs, several experiments to create IASI RGBs over Polar Regions and global coverage were carried out. After the launch of METOP-B, METOP-A and METOP-B IASI datasets can be used together to build global coverage airmass RGB images as shown in Figure 8 and Figure 9. Once the brightness temperatures for the channels involved in the IASI RGB are read from the hyperspectral files, actual IASI RGB images can be generated. The computational cost of RGB imagery generation is very low and, if adequate software package would be available, then hyperspectral RGB images would be generated in near real time. This issue is addressed in Section 6.

The IASI L1 files used to built the IASI airmass RGB in Figure 8 and 9 correspond to 20th February 2013 morning. This case study was selected because a tropical cyclone named Haruna was near Madagascar coasts and METOP-A and METOP-B were both available. The images in Figure 8 could be one example of the interactive use of hyperspectral Level 1 data as image fields by forecasters and could also be used as one excellent background for NWP field displays.

A video showing the global coverage and the interactive use by forecaster is available but there is not available in one web page. A video showing the global coverage and the interactive use by forecasters is available upon request to *mmartinezr@aemet.es*

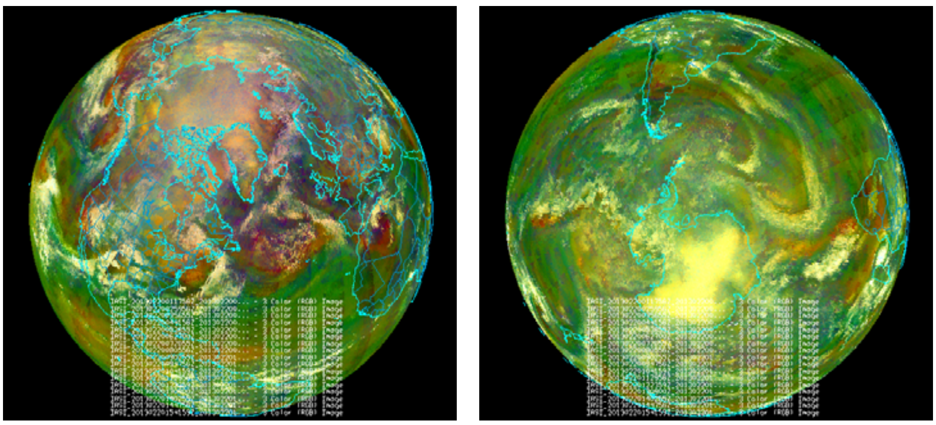

Figure 8: METOP-A and METOP-B IASI global airmass RGB for day 20th February 2013 morning using McIDAS-V Globe display.

The process to generate images in Figure 8 and Figure 9 are described in Section 6.

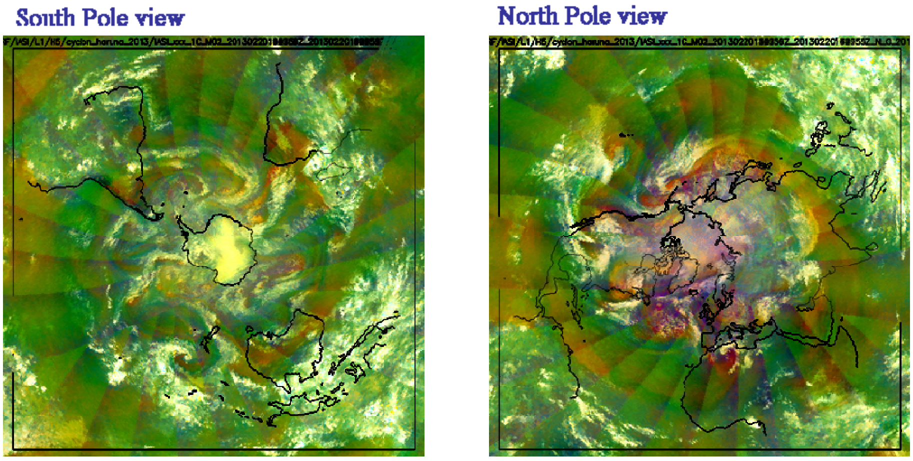

Figure 9: *METOP-A and METOP-B IASI global airmass RGB for day 20th February 2013 morning using IDL with transparent PNGs for polar displays.*

4.3 ACTUAL AIRMASS RGB IMAGES WITH OTHER HYPERSPECTRAL INSTRUMENTS

A similar process as the one described above for searching IASI channels equivalent to SEVIRI channels could be repeated for other hypespectral instruments. In Figure 10, one example using actual AIRS data is shown.

This demonstrates the possibility to generalize the RGBs construction to other instruments like CrIS on board NPP-SUOMI. The combined use of RGB images from several hyperspectral instruments could improve monitoring regions not covered now by RGB images from geostationary satellites; especially over Polar Regions due to the high revisiting frequency.

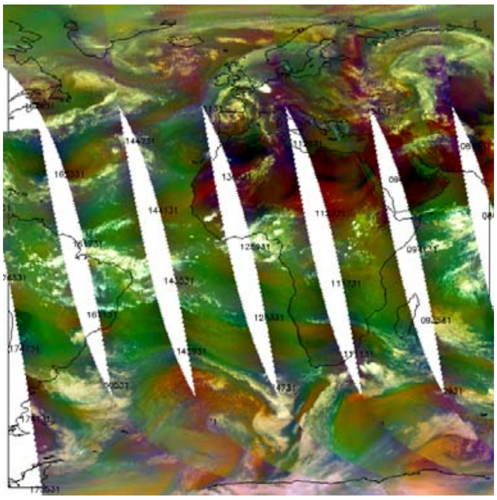

Airmass RGB	AIRS Channel	Range	g
RED	$AIRS_{6.99519}$ -$AIRS_{7.41335}$	-25… .+0K	1.0
GREEN	$AIRS_{9.66956}$ -$AIRS_{10.8032}$	-40… ..+5K	1.0
BLUE	$AIRS_{6.99519}$	+243…… 208K	1.0

Figure 10: AIRS airmass RGB for day 25th May 2009 afternoon using actual AIRS HDF files (first CWG case study strong convection on Europe).

4.4 ACTUAL IASI DUST RGB

The MSG dust RGB has been widely used for dust and sand storm monitoring. The recipe to built the dust RGB is shown in Table 5.

DUST (night & day)					
RGB colour plane	channel (difference)	MIN	MAX	GAMMA	Prominent features
R	12.0 - 10.8	-4 K	+2 K	1.0	Dust (over land) Thin Ci Contrails
G	10.8 - 8.7	0 K	+15 K	2.5	
B	10.8	261 K	289 K	1.0	

Table 5: MSG dust RGB construction composite (source best_practices.pdf document)

In Figure 11, it can be seen that the IASI dust RGB image is able to detect the dust storm over the Sahara desert and the Canary Islands. The first direct use of an IASI dust RGB could be to help in the subjective selection of clear and dust contaminated pixels for further study of dust contaminated IASI spectra. They could be archived and later used as a collection of spectral probes to train automatic classifications of clear or dusty IASI spectra.

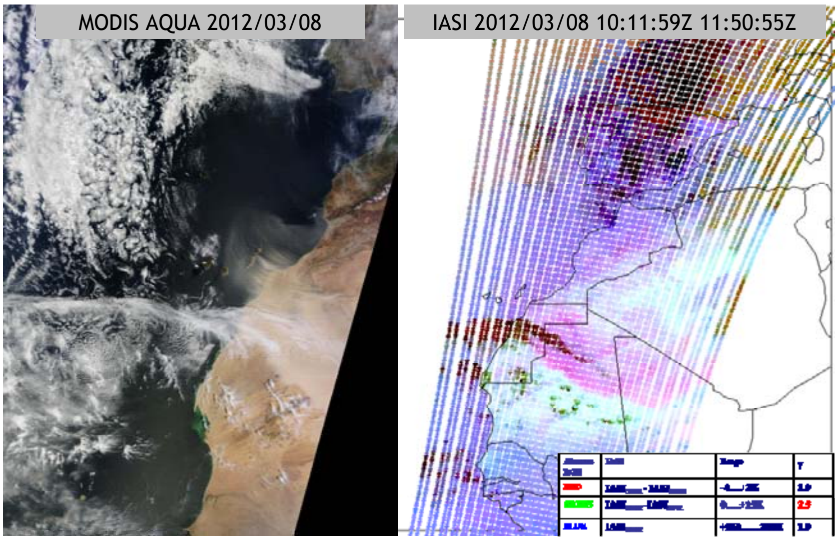

Figure 11: (left) MODIS true color RGB in one strong dust storm on the Sahara reaching the Canary Islands, (right) IASI dust RGB for the same case.

MSG dust RGBs have also been used for volcanic eruption monitoring (as example in the Iceland volcanoes eruptions). In the same way, IASI dust RGB images can also be used for global monitoring of volcanic ash and SO_2 with a single common instrument; with the added advantage that on Polar Regions the low zenith angles also improves the detection.

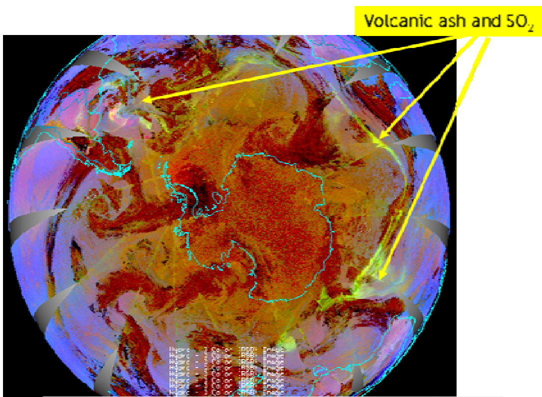

Airmass RGB	IASI	Range	γ
RED	$IASI_{12.0736}$ - $IASI_{10.9800}$	-4….+2K	1.0
GREEN	$IASI_{10.9800}$ -$IASI_{9.00441}$	0…..+15K	2.5
BLUE	$IASI_{10.9800}$	+261……289K	1.0

Figure 12: IASI dust RGB showing the volcanic ash and SO_2 from the eruption of Chilean Puyehue-Cordon-Caulle Volcano from 9th June 2011 22:24Z to 10th June 2011 10:35.

As example the actual IASI dust RGB image from the eruption of the Chilean Puyehue-Cordon-Caulle Volcano using METOP-A IASI L1 data for 9th June 2011 22:24Z to 10th June 2011 10:35Z is shown in Figure 12. The actual IASI dust RGB image has been created using McIDAS-V on Globe display and IASI L1 HDF-5 files from EUMETSAT UMARF.

5. SEARCH OF NEW MTG-IRS RGBs

The search of new MTG-IRS RGBs without MSG RGB heritage would be the next step in order to take full advantage of the added value of MTG-IRS spectral resolution with respect to MSG SEVIRI. Going further, other products, apart from RGB imagery, should be studied in the future.

As an early idea and with the target to demonstrate the possibility to search new MTG-IRS RGBs without MSG RGB heritage, in 2010 it was built an early RGB with direct application for Nowcasting. This new RGB product tries to monitor ozone and water vapour vertical distribution (Martinez et al., 2010a).

Ozone monitoring could be used as a proxy for the sinking of the tropopause and vorticity maximums. The vertical distribution of water vapour is a critical ingredient to trigger convection. In the NWC SAF PGE13 SPhR product several precipitable water layers are defined; the layers are named BL, ML and HL. BL is the low layer precipitable water and it is defined as the precipitable water for a layer between surface pressure to 850 hPa. ML is the medium levels precipitable water and is defined as the precipitable water for a layer from 850 hPa to 500 hPa.

BL and ML fields from NWC SAF PGE13 SEVIRI Physical Retrieval product (SPhR) product have been proved to be useful to search and monitor regions that are susceptible to trigger convection (Martinez et al., 2010b).

NWC SAF PGE13 SPhR product training and validation tools were used to calculate Total ozone in Dobson units (TOZ), BL and ML from the ECMWF analysis profiles for 25th May 2009 at 12Z.

Linear regressions between every pair of synthetic MTG-IRS BT (or synthetic IASI BTs) and every one of the above ECMWF fields were calculated. Then the RMSE and Correlation matrices were obtained by calculation of correlation and RMSE after applying the regression between every pair of synthetic MTG-IRS BTs and each one of the parameters (TOZ or BL or ML). In Figure 13 the correlation matrix for the Total Ozone and the linear regressions each two MTG-IRS channels is shown as an example.

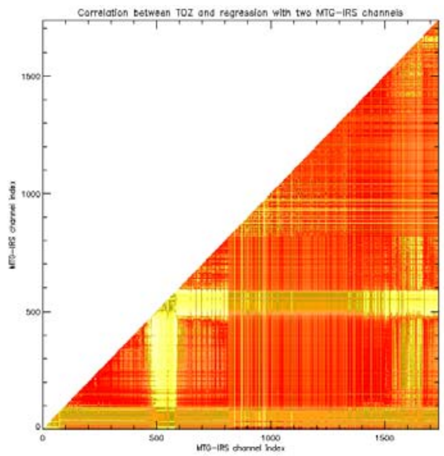

Figure 13: Correlation matrix between total ozone of ECMWF GRIB file and a linear regression made with each two RTTOV MTG-IRS channels BT

Next step consist in finding the optimal regressions which simultaneously satisfies to have low RMSE and high correlation. Due to the huge size of the matrices and the large variability between near positions on the matrices, an automatic process must be used. A “fuzzy-logic” like scheme was used to search for the optimal regression which simultaneously satisfies to have low RMSE and high correlation. The scheme is based on the following steps performed with the correlation and RMSE matrices for each nowcasting parameter:

- First, the normalized correlation matrix is calculated by fixing to zero those positions with correlation lower than the mean correlation value and normalize the remaining in [0, 1] range.
- Second, the normalized RMSE matrix is calculated by fixing to zero those positions with RMSE greater than the mean RMSE value and normalizing the remaining in [0, 1] range in such way that the lowest RMSE position is assigned the normalized value of 1.
- Finally, the two normalized matrices are multiplied and the regression for the position with the maximum value in the product matrix is the combination chosen to build the optimal regression.

This optimal regression for one parameter is a combination of MTG-IRS channels having simultaneously very high correlation and very low RMSE.

This process has been repeated for ML, TOZ and BL parameters. Table 6 shows the optimal regressions and the channels that have been used to generate the synthetic MTG-IRS RGB image in Figure 14.

Physical parameter	1st MTG-IRS channel number *(0-based)*	λ of 1st MTG-IRS channel number *(μm)*	2nd MTG-IRS channel number *(0-based)*	λ of 2nd MTG-IRS channel number *(μm)*	Regression coefficients ($\alpha + \beta_1 * BT_{1st} + \beta_2 * BT_{2nd}$)		
					α	β_1	β_2
ML layer (precipitable water 850 to 500 hPa)	1717	4.6243	1539	4.8751	-10.34	5.25	-5.13
TOZ (Total Ozone)	465	10.0900	457	10.1458	971.63	-235.7	232.57
BL layer (precipitable water P_{sfc} to 850 hPa)	1506	4.9246	802	8.3247	-74.82	-17.07	17.37

Table 6: List of MTG-IRS channels used in the regressions to make the new MTG-IRS RGB.

The result of the regressions for *MTG-IRS* ML, MTG-IRS TOZ and MTG-IRS BL using as input the pair of channels from the 2nd and 4th columns of the Table 6 and the regression coefficients of the 6th column are shown in Figure 14.left. When the three images from Figure 14.left) are remapped over SEVIRI projection and combined in a RGB, it is obtained the MTG-IRS RGB image of Figure 14.right. The byte scaled MTG-IRS ML precipitable water regression has been used for the red component. The byte scaled MTG-IRS TOZ regression has been used for the green component. The byte scaled MTG-IRS BL precipitable water regression has been used for blue component.

In Figure 14.right, it can be seen the humid regions as purple or pink colors and the high ozone concentration regions in green pixels (which is a proxy of vorticity maximum). In Europe it can be seen the humid region over France and Germany and the green tone of high ozone region over Spain and west part of France. These facts indicate the presence of ingredients needed for convection triggering. More information on the convection event over Europe can be found in (Martinez et al., 2010b) and at the Convection Working Group web.

Since the values of β_1 and β_2 regression coefficients are similar in absolute value, a simple difference of channels could be considered to be used in the final design of the MTG-IRS RGBs; this would simplify the MTG-IRS RGBs calculations. This would be done as a follow on work once noise levels and further studies with a greater MTG-IRS dataset would have been carried out.

This algorithm could be generalized to find more combinations with other parameters. Also, other algorithms instead of just linear regressions (like better statistical algorithms, neural neworks, etc) could be tested in future.

Other issue to consider is that in this early example the search is made between all MTG-IRS channels but for future operational algorithms the search should be restricted to a set of selected MTG-IRS channels. In future works, it should be avoided from the search those MTG-IRS channels with high noise levels or not recommended by any spectroscopical reason.

Since IASI and MTG-IRS sensors can resolve spectral bands for several chemical species, other research line would be to obtain RGB images for other species like, for example, SO_2.

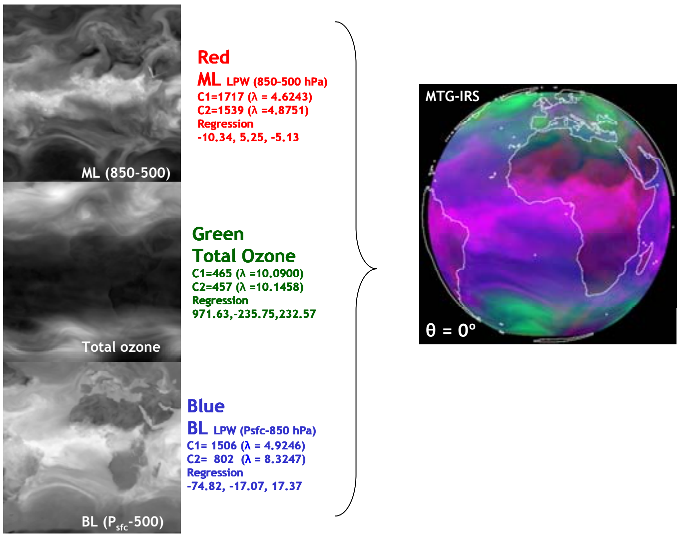

Figure 14: New RTTOV MTG-IRS RGB. It has been built using byte scaled regressions of two synthetic MTG-IRS channels and some meteorological fields. (top left red) regression of two MTG-IRS synthetic BTs and ML, (medium left green) same but with Total ozone, (bottom left blue) same but with BL. Synthetic MTG-IRS and BTs from ECMWF analysis 25th May 2009 at 12Z with 0º zenith angle.

This algorithm works well with synthetic MTG-IRS BTs, but before applying it to actual data a previous bias correction of the BTs would be needed. The work described here should be seen as an early test. Because the profile dataset is small, no noise and no clouds have been introduced in the simulations. It just tries to illustrate the way to proceed. Further work should consolidate this.

6. OPERATIONAL IMPLEMENTATION ISSUES

The lack of proper software tools able to automatically generate actual IASI RGB images using the EUMETCast or UMARF files makes impossible an operational generation and use of these images nowadays.

To get interactive use of hyperspectral data an agreement between user tools and EUMETSAT formats is needed. The process followed to generate actual IASI RGB images showed in Figures 8, 9 and 12, is described below. With this information one can spot some of the issues that users would find in order to build their own actual IASI RGB imagery.

Figures 8 and 12 were generated with the free software McIDAS-V *(http://www.ssec.wisc.edu/mcidas/software/v/).*

The image shown in Figure 12 was the first actual IASI RGB image generated. It was created with McIDAS-V tool using the IASI L1 files in HDF-5 format downloaded from UMARF. When downloading files form UMARF, it is not possible to choose a list of selected channels. The whole orbit with all channels must be downloaded. This means that, for example, to generate the image in Figure 12 eight IASI HDF-5 files larger each one than 2 GB must be managed.

Once the IASI HDF-5 files are available, the orbit to orbit superposition was needed to create the joint image. Since this image processing was built both manually and interactively, and 15 minutes were needed to process each HDF5, to obtain an image like the one shown in Figure 12 several hours are needed. The steps taken for each one of the IASI files to build the image showed in Figure 12 using the McIDAS-V tool are the following:

a) load interactively the first 2GB HDF-5 IASI L1 file. Due to the weight of this file, this step can take several minutes

b) interactively create the regression for the red RGB component using a graphical tool called “Linear Combination”. When using this tool, the channels must be selected manually, moving a colour line along the spectra. It takes some time to change channel selection

c) steps a) and b) must be repeated for the green and blue components of the RGB product

d) compute the RGB product using McIDAS-V software. Globe display is used is used to that end

e) unload HDF-5 IASI L1 file in order to free memory, load next file and repeat the process

Note 1: IASI L1 in netCDF format downloaded from UMARF can not be used due to a bug: several parameters are not filled in these netCDF files.

Note 2: McIDAS-V has a tool to make some part of the above process with Jython(Python based on Java) but I don’t have enough knowledge to do it.

Figure 8 was created writing an internal IDL conversion procedure to write intermediate netCDF files with reduced sized and adapted for the RGB formula tool of McIDAS-V. This process reduces the huge amount of time needed to work with the more than twenty METOP-A and METOP-B IASI files required to get Global Coverage interactively.

The IDL conversion program performs the following process for each one of the HDF-5 IASI files:

a) Reading of HDF-5 IASI file containing all IASI channels

b) Conversion from radiances to BTs and selection of just those equivalent channels used to build IASI airmass RGB images

c) Writing on a file with netCDF format just the channels named with the names needed by the McIDAS-V RGB tool for airmass RGB

d) Adding latitude and longitude data to the NetCDF files for an easier navigation.

This process is illustrated in Figure 15. The smaller size of these NetCDF files and the fact that the IASI BTs for each channel are named accordingly with McIDAS-V airmass RGB formula reduced the time to process each file with one orbit to less than three minutes.

This test demonstrates that if UMARF would allow selection of IASI channels or if suitable software would be developed then actual IASI RGB generation could be run interactively by users.

This process just illustrates that with the adequate software the generation could be made interactively by users.

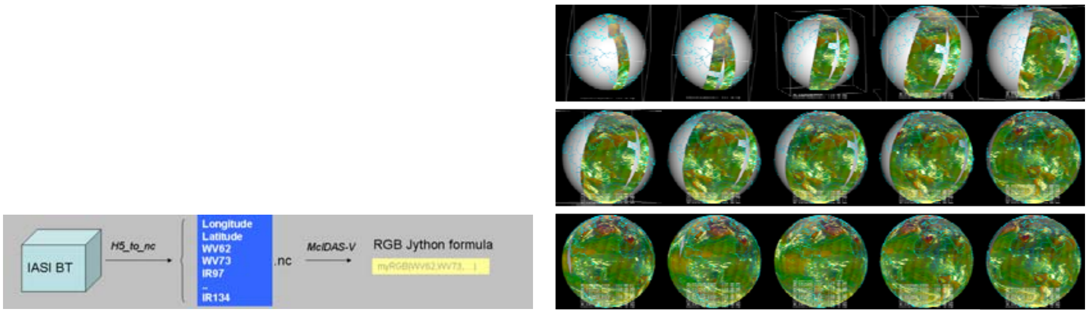

Figure 15: Process to faster generation of interactive actual IASI RGB images with McIDAS-V.

Images in Figure 9 are an example of IASI L1 HDF-5 files exploitation by using batch tools. PNG files containing one IASI orbit and transparency out of the orbit with the same projection and size, were written using an IDL program. Any image display tool (like PowerPoint, a web browser or ImageMagick) can be used to put together all the transparent PNG files and get a final combined image. After the proper alignment of the images the effect of Polar coverage is reached. The transparent part of the image allows the view of the non-transparent part of images located behind it.

In Figure 16 an example of one of these images with one orbit and transparency out of the orbit is shown. Each one of these PNG images is written on 4 bytes per pixel. These PNG images are RGBA type; where A means a degree of transparency. So the meaning of the bytes is red, green, blue and transparent. Red, green and blue bytes are used to build the RGB image along the IASI orbit and the transparent byte is used to declare the pixels out of the orbit as transparent.

Although the example shown in Figure 9 is just an early example, it demonstrates that actual IASI RGB imagery generation is possible. In order to get near real time generation, future work could be conducted to the incorporation of hyperspectral RGB imagery generation to operational software packages such as NWC SAF/PPS or CIMSS/CSPP.

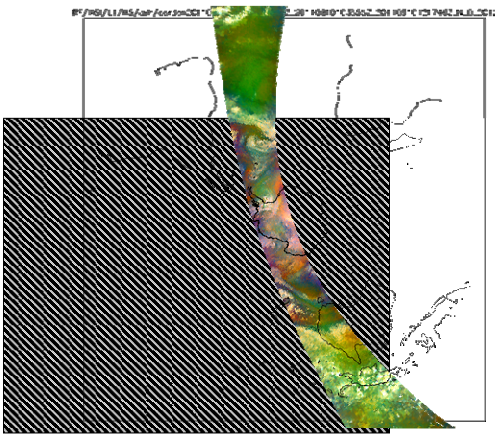

Figure 16: RGBA PNG example. The 4 bytes RGBA PNG format has been used. For every pixel there are 4 bytes (red, green, blue, transparency). The pixels out of the orbit are fixed to 0 and transparency = 0 means full transparent pixel.

7. CONCLUSIONS

The studies described here have been created to achieve use and generation experiences with hyperspectral data using IASI as proxy of MTG-IRS L1.

Near real time RGB images are very useful for nowcasting purposes. In this document, the pioneering activity, initiated in 2010, to build RGB images from hyperspectral data have been shown. As a first incursion, some MSG RGB imagery, widely used by forecasters, have been obtained here, derived from both synthetic and actual hyperspectral data.

Actual IASI RGB images have been generated and compared to MSG RGB ones; it has been shown the advantages and limitations. RGB imagery generated from low earth orbit hyperspectral instruments like AIRS, IASI and CrIS could be used nowadays operationally in nowcasting, especially over Polar Regions. The use of hyperspectral RGB images could be started following the heritage of MSG-SEVIRI RGB images.

The main conclusion is the possibility of the generalization of RGB images technique to hyperspectral instruments. New RGB images from hyperspectral L1 data could be developed and used operationally with future hyperspectral geostationary satellite instruments like MTG-IRS.

These early tests should be understood as an example against the preconceived idea that MTG-IRS L1 is only useful for NWP or generation of L2 products. Hyper spectral RGB imagery examples presented in this document were introduced as one counterexample to the question: Is it possible the use of IRS L1 in Nowcasting? The IASI and MTG-IRS RGB imagery generation should be understood as positive answer, there is at least one starting point for the use of MTG-IRS Level 1 for nowcasting purposes.

These, today only naive applications, could be made available. But as another conclusion of the experiences described in this document, an recommendation could be given to EUMETSAT to synchronize file formats with user software tools to avoid the chicken-egg problem no software-no users.

A web site collecting all these studies, software and information should be created. Since the main goal of these studies has nowcasting purposes, first option should be the NWC SAF web server *http://www.nwcsaf.org*

7.1 FUTURE WORKS

Due to the low number of IASI spectra and synthetic MTG-IRS spectra used in this paper, further studies should be carried out for each one of these early ideas with higher number of IASI spectra and in more cases.

Other activities performed in 2013 are described in (Martinez and Calbet, 2013). Other early brainstorm ideas for direct use of IASI L1 data are shown below:

a) use of the separated local maxima and local minima envelope lines to represent IASI spectra in order to allow easy comparison between spectra from different spatial or time coordinates.

b) one representation of the “peaks” and “valleys” as a potential “spectral-gram”,

c) loops using a selection of channels on "CO_2 or WV" absorption bands with channels peaking from the top of the atmosphere gradually down to the surface,

d) more examples of search for new RGBs

e) some early tests on the generation of Principal Component's images with direct physical interpretation.

All of them should be consolidated in future. A roadmap of future developments for MTG-IRS L1 and MTG-IRS L2 is shown in Figure 17.

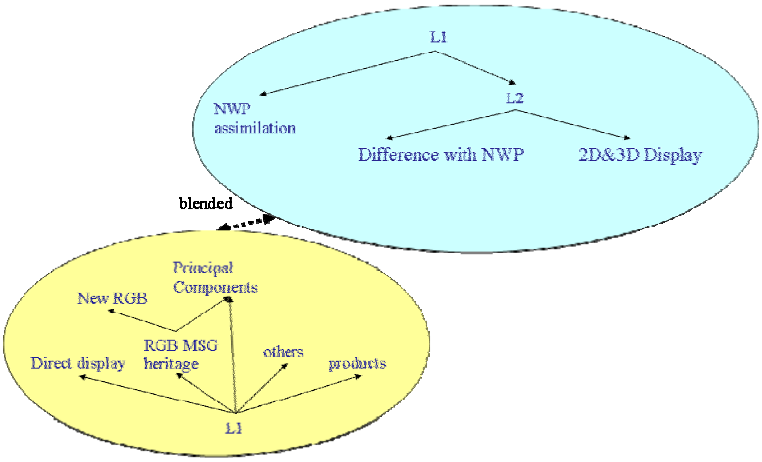

Figure 17: Map of developments from MTG-IRS L1 and L2.

8. ACKNOWLEDGEMENTS

Xavier Calbet (EUMETSAT)

MIST group.

9. REFERENCES

Eyre, J.R., 1991. *A fast radiative transfer model for satellite sounding systems.* ECMWF Res. Dep,Tech. Mem. 176. ECMWF,Reading, United Kingdom, 28 pp.

Li, J. and Huang, H. L., 1999*: Retrieval of atmospheric profiles from satellite sounder measurements by use of the discrepancy principle.* Appl. Optics, Vol. 38, No. 6, 916-923.

Li, J.; et al., 2000. *Global soundings of the atmosphere from ATOVS measurements: The algorithm and validation*. J. Appl. Meteorol., Vol 39, pp 1248 – 1268.

Martínez M.A.; Li, J. 2009. *First operational results of the NWCSAF/MSG PGE13 MSG Physical Retrieval algorithm.* Proc. of the 2009 EUMETSAT Conference, Bath, United Kingdom.

Martínez M.A., X. Calbet, Prieto J., Tjemkes S. 2010a. *Use of synthetic RGB images in training.* Proceedings of the 2010 EUMETSAT Meteorological Satellite Conference, Cordoba, Spain.

Martinez, M A.; Li, J.; Romero, R. 2010b. *NWCSAF/MSG PGE13 Physical Retrieval product version 2010.* Proceedings de EUMETSAT 2010 Conference.

Martinez M.A., Calbet X., 2013. *Innovative ideas for using the hyperespectral level 1 data of the next geostationary MTG-IRS in nowcasting.* Proc. of the 2013 EUMETSAT Conference, Vienna, Austria.

Saunders, R.; Matricardi, M. and Brunel, P., 1999. *An improved fast radiative transfer model for assimilation of satellite radiance observation.* Quart. J. Roy. Meteor. Soc., Vol. 125, 1407–1425.

Sieglaff J.M., Schmit T.J., Menzel W.P., Ackerman S.A. (2009). *Inferring Convective Weather Characteristics with Geostationary High Spectral Resolution IR Window Measurements: A Look into the Future.* J. of Atmospheric and Oceanic Technology Vol 26, Pages 1527-1541.

Tjemkes, S. and Calbet, X., 2008. *IASI to MTG-IRS conversion tool.* Personal communication